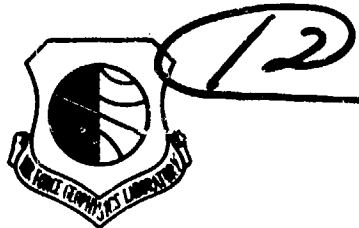


ADA102908

LEVEL ✓

AFGL-TR-81-0108
INSTRUMENTATION PAPERS, NO. 302



**Attitude Determination of a Spinning
and Tumbling Rocket Using Data
From Two Orthogonal Magnetometers**

SHU T. LAI

8 April 1981

DTIC

AUG 17 1981

H

Approved for public release; distribution unlimited.

SPACE PHYSICS DIVISION PROJECT 7661
AIR FORCE GEOPHYSICS LABORATORY
HANSCOM AFB, MASSACHUSETTS 01731

AIR FORCE SYSTEMS COMMAND, USAF



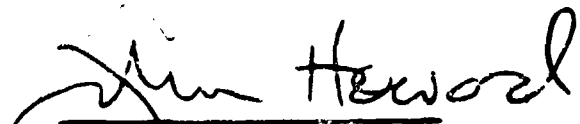
81 8 17 055

FILE COPY

This report has been reviewed by the ESD Information Office (OI) and is releasable to the National Technical Information Service (NTIS).

This technical report has been reviewed and is approved for publication.

FOR THE COMMANDER



Jim Haworth
Chief Scientist

Qualified requestors may obtain additional copies from the Defense Technical Information Center. All others should apply to the National Technical Information Service.

(14) AFGL-TR-X-414
AFGL-TR-342

(12)

Unclassified

SECURITY CLASSIFICATION OF THIS PAGE (When Data Entered)

REPORT DOCUMENTATION PAGE		READ INSTRUCTIONS BEFORE COMPLETING FORM
1. REPORT NUMBER AFGL-TR-81-0108 ✓	2. GOVT ACCESSION NO. AD-A102908	3. RECIPIENT'S CATALOG NUMBER
4. TITLE (INCLUDE GRADE, MODEL, ETC.) ATTITUDE DETERMINATION OF A SPINNING AND TUMBLING ROCKET USING DATA FROM TWO ORTHOGONAL MAGNETOMETERS.		5. TYPE OF REPORT & PERIOD COVERED Scientific Interim
6. AUTHOR(s) Shu T. Lai	7. PERFORMING ORGANIZATION NAME AND ADDRESS Air Force Geophysics Laboratory (PHK) Hanscom AFB Massachusetts 01731	
8. CONTROLLING OFFICE NAME AND ADDRESS Air Force Geophysics Laboratory (PHK) Hanscom AFB Massachusetts 01731		10. PROGRAM ELEMENT, PROJECT, TASK AREA & WORK UNIT NUMBERS 62101F 76610902
11. MONITORING AGENCY NAME & ADDRESS (If different from Controlling Office)		12. REPORT DATE 8 April 81
		13. NUMBER OF PAGES 32
14. DISTRIBUTION STATEMENT (DoD Report)		15. SECURITY CLASS. (of this report) Unclassified
		15a. DECLASSIFICATION/DOWNGRADING SCHEDULE
16. SUPPLEMENTARY NOTES Part of the work was performed under contract F19628-C-0018 with Boston College.		
17. KEY WORDS (Continue on reverse side if necessary and identify by block number) Attitude Local vertical coordinate Spinning Trajectory plane Tumbling Magnetic field line Rocket Moon direction Magnetometer		
18. ABSTRACT (Continue on reverse side if necessary and identify by block number) > This technical note reports on the attitude determination of Air Force Rocket No. A31.603 on which an ion emission experiment was performed. Two orthogonal magnetometers, one facing forward along the rocket spin axis and the other facing sideways, provide magnetic field component data. The bias-offset and scaling (signal conversion) factor are not given, but can be determined in a sinusoidal approximation. The algorithm used for generating magnetic pitch angles is discussed and an error analysis is provided.		

DD FORM 1 JAN 73 1473

Unclassified

SECURITY CLASSIFICATION OF THIS PAGE (When Data Entered)

409578

Unclassified

SECURITY CLASSIFICATION OF THIS PAGE(When Data Entered)

20. (Cont)

In a local vertical coordinate system, two sets of elevation angles are found for the tumbling rocket, and the set that satisfies an initial condition exactly is the correct one. The deviation of the rocket tumbling plane from the vertical plane can be determined at the times of closest encounter of the magnetic field vector and rocket vector. The deviation at all times can be approximately determined by sinusoidal curve fitting with tumbling frequency. The angles between the rocket vector and moonlight vector during the instants of moonviews at the onboard camera are also calculated.

Unclassified

SECURITY CLASSIFICATION OF THIS PAGE(When Data Entered)

Preface

It is a pleasure to thank Herbert A. Cohen for his initiation, guidance, and encouragement; William A. Burke provided invaluable help in the calculation of moon directions, and kindly read the manuscript with encouraging comments; Krishin H. Bhavnani kindly provided a computer computation on moon directions; and Brian Sullivan and Malcom Chamberlain provided the data listed in References 2 and 4 respectively.

Part of this work was performed under AFGL Contract F19628-79-C-0018 while the author was with Boston College.

Accession For	NTIS GRA&I	<input checked="" type="checkbox"/>
	DTIC T&E	<input type="checkbox"/>
	Unannounced	<input type="checkbox"/>
Justification		
By _____		
Distribution		
Available by Codes		

A		

Contents

1. INTRODUCTION	7
2. BIAS OFFSET	8
3. SCALING FACTOR	9
4. ASPECT ANGLE	10
5. TUMBLING AND SPINNING ROCKET	10
6. ERROR ANALYSIS ON ASPECT ANGLE ALGORITHM	11
7. THE PROBLEM OF ATTITUDE DETERMINATION OF ROCKET AXIS	12
8. ZEROOTH ORDER APPROXIMATION	13
9. ROCKET ELEVATION AND AZIMUTH ANGLES	14
10. MOON DIRECTION	15
REFERENCES	21
APPENDIX A: Attitude Data of Rocket No. A31, 603	23

Illustrations

1. Local Vertical Coordinate System	14
2. Rocket Attitude in the Plane of Rocket Trajectory	16

Illustrations

3. Rocket Elevation Angle, Azimuth Angle, and the Angle Between Rocket and Moonlight	18
4. Relation of Rocket and Moonshine Directions	18

Tables

1. Ephemeris Data of Moon and Launch Site	16
2. Rocket Attitude Angles During Moon View Times	19

Attitude Determination of a Spinning and Tumbling Rocket Using Data From Two Orthogonal Magnetometers

I. INTRODUCTION

This work was motivated by data obtained on Air Force scientific rocket No. A31.603. Electron and ion beam experiments¹ were carried out on the rocket. In order to analyze and interpret the scientific data, it is necessary to know the attitude of the rocket during the instants of beam emissions. Of particular importance is the angle between the rocket and geomagnetic field lines, because the presence of the geomagnetic field gives rise to anisotropic electron motion. The electrons move easily along, but with difficulty across the geomagnetic field. Furthermore, there are indications^{2,3} that the magnitude of return current is less for a beam emitted downwards along the magnetic field.

Other interests also motivated this work. The standard technique of attitude determination with magnetometer data requires data from three orthogonal

(Received for publication 31 March 1981)

1. Cohen, H.A., Sherman, C., and Mullen, G. (1979) Spacecraft charging due to positive ion emission: an experimental study. Geophys. Res. Lett. 6(No. 6):515.
2. Winckler, J.R. (1980) The application of artificial electron beams to magnetospheric research. Review of Geophysics and Space Physics, 18:659-682.
3. Jacobsen, T.A., and Maynard, N.C. (1980) Polar 5—an electron accelerator experiment within an aurora 3. Evidence for significant spacecraft charging by an electron accelerator at ionospheric altitudes. Planet. Sp. Sci. 28:291-307.

magnetometers, the magnetometer telemetry signal conversion factors being known from pre-launch calibration. However, when only data from two orthogonal magnetometers are available and the conversion factors are not given, it becomes a challenging problem whether the attitude can still be estimated in a local vertical coordinate system. For an object tumbling slowly, compared with its spinning, in a vertical plane with small sinusoidal variations, a method is offered for solving this problem.

The position \underline{p} of the spacecraft and the Earth's magnetic field vector \underline{B} at that position are given. The magnetometer data (hereafter abbreviated as m. d.) are known to be approximately linearly related to the true magnetic data \underline{B} by:

$$(\underline{M} - \underline{D})\underline{S} = \underline{B}$$

where \underline{M} , \underline{D} , and \underline{S} are m. d., bias offset, and scaling factor respectively. For a triaxial magnetometer set, the three components of \underline{M} can be obtained. If only two magnetometers are available, additional techniques have to be devised. The main objective is to determine the directions of the magnetometers with respect to the local vertical coordinate system, those with respect to the spacecraft coordinate system being given.

2. BIAS OFFSET

If the m. d. varies in a simple sinusoidal manner and then for a sufficiently long period in a steady state, the bias offset can be determined as the mean of the m. d. in that period, because

$$\langle A \sin \omega(t - t_0) + D \rangle = \langle A \sin \omega(t - t_0) \rangle + D \approx D.$$

If more than one significant frequency is present in the steady state time series, the bias offset can be determined in the same manner, because

$$\lim_{t \rightarrow \infty} \langle \sum_i A_i \sin \omega_i(t - t_0) + D \rangle = \sum_i \langle A_i \sin \omega_i(t - t_0) \rangle + D \approx D.$$

This method applies to the time series of each magnetometer.

If the time span of available data is short, such as three periods ($3 \times \omega^{-1}$) or less, for example, then the offset D has to be determined by least square curve fitting, if good accuracy is desired. For rigid bodies, sine functions with known frequencies are usually suitable for fitting purposes. The frequencies can be computed by means of fast Fourier transform or maximum entropy methods.

3. SCALING FACTOR

After removing the bias offset, D , the magnetometer data $\{M\}$ become directly proportional to the magnetic field components $\{B\}$. If data from only two magnetometers were available, it would not be possible to derive exact knowledge of the three dimensional vector $\underline{M}(t)$ at any time t . However, in an ideal situation—that is, when the spin vector of the vehicle remains constant in direction with respect to an inertial coordinate system in which the magnetic field lines are at rest—the scaling factor can be determined as follows.

Let $M_1(t)$ and $M_2(t)$ be available during a spin period, $M_3(t)$ being unavailable. Let $M_1(t)$ be the measurement in the spin direction. The Earth's magnetic field $\underline{B}(t)$ is assumed constant in the space and period considered. With the vehicle spinning about the one-direction, the magnetometer readings $\{M(t)\}$ at time t are given by

$$[\underline{M}(t)] = \begin{bmatrix} 1 & 0 & 0 \\ 0 & \cos \phi(t) & \sin \phi(t) \\ 0 & -\sin \phi(t) & \cos \phi(t) \end{bmatrix} [\underline{M}(t_0)] \quad (1)$$

where

$$|\underline{B}| = S \left\{ M_1^2(t_0) + M_2^2(t_0) + M_3^2(t_0) \right\}^{1/2}, \quad (2)$$

S being the scaling factor.

In a spin period, the extremum value of $M_2(t)$ is given by

$$\partial M_2(t)/\partial \phi(t) = 0$$

which, using Eq. (1), gives

$$\phi(t) = \tan^{-1} \left[M_3(t_0)/M_2(t_0) \right]$$

and

$$\text{Max}[M_2(t)] = \left\{ M_2^2(t_0) + M_3^2(t_0) \right\}^{1/2} \quad (3)$$

so that

$$\left\{ M_1^2(t) + \text{Max}^2 [M_2(t)] \right\}^{1/2} = \left\{ M_1^2(t_0) + M_2^2(t_0) + M_3^2(t_0) \right\}^{1/2}.$$

Therefore,

$$|\underline{B}| = S \left\{ M_1^2(t) + \text{Max}^2 [M_2(t)] \right\}^{1/2}. \quad (4)$$

Thus, despite the lacking of $M_2(t)$ data at any time t , the scaling factor S can be determined, using Eq. (4), if the value $|\underline{B}|$ is known by using standard model calculations or other appropriate data if available.

4. ASPECT ANGLE

The aspect angle $\alpha_i(t)$ subtended by the i th magnetometer vector with the Earth's magnetic field line \underline{B} at time t is given by

$$\alpha_i(t) = \cos^{-1} \left\{ \frac{\underline{S} M_i(t) \cdot \underline{B}(t)}{|\underline{B}(t)|^2} \right\}. \quad (5)$$

Thus,

$$\alpha_i(t) = \cos^{-1} \left\{ \frac{M_i(t)}{\sqrt{M_1^2(t) + \text{Max}^2 [M_2(t)]}} \right\}. \quad (6)$$

Of particular interest for Rocket A31.603 is magnetometer No. 1, which points forward along the rocket axial vector, the spin axis being about coincidental with the geometric axis. Thus, the aspect angle $\alpha_1(t)$ gives the angle subtended by the rocket axis with the \underline{B} line at the rocket's location.⁴

5. TUMBLING AND SPINNING ROCKET

In general situations, the spin vector of a vehicle does not remain constant in direction with respect to an inertial coordinate system. For a pure tumbling and spinning vehicle, the magnetometer data $\{M(t)\}$ measured on the vehicle at time t are given by

$$\begin{bmatrix} \underline{M}(t) \end{bmatrix} = \begin{bmatrix} 1 & 0 & 0 \\ 0 & \cos \phi(t) & \sin \phi(t) \\ 0 & -\sin \phi(t) & \cos \phi(t) \end{bmatrix} \begin{bmatrix} \cos \theta(t) & 0 & \sin \theta(t) \\ 0 & 1 & 0 \\ -\sin \theta(t) & 0 & \cos \theta(t) \end{bmatrix} \begin{bmatrix} \underline{M}(t=0) \end{bmatrix} \quad (7)$$

4. SUA/AFGL (1979) Data Report Rocket No. A31.603.

where the tumbling axis is the y-axis in the inertial system and the spinning axis is the x-axis in the spacecraft system. At time $t = 0$, $\theta(t)$ and $\phi(t)$ are defined as 0. In a spinning period, the maximum value of $M_2(t)$ is measured when $\phi(t)$ satisfies the following equation, at $t = t_m$,

$$\frac{\partial}{\partial \phi} \left[-\sin \theta \sin \phi M_1(0) + \cos \phi M_2(0) + \cos \theta \sin \phi M_3(0) \right] = 0$$

which gives, using Eq. (7),

$$\text{Max} [M_2(t)] = \left\{ M_2^2(0) + \cos^2 \theta(t_m) M_3^2(0) + \sin^2 \theta(t_m) \right. \\ \left. M_1^2(0) - 2 \cos \theta(t_m) \sin \theta(t_m) M_1(0) M_3(0) \right\}^{1/2}. \quad (8)$$

If the spin frequency is much higher than the tumble frequency, then $\theta(t_m)$ would not be too different from $\theta(t=0)$, which is zero. Thus,

$$\lim_{\theta \rightarrow 0} \text{Max} [M_2(t)] = \left\{ M_2^2(0) + M_3^2(0) \right\}^{1/2}, \quad (9)$$

which reduces to Eq. (3), the result for no tumble case.

6. ERROR ANALYSIS ON ASPECT ANGLE ALGORITHM

For low tumble frequency/spin frequency ratio, the aspect angle $\alpha_i(t)$ subtended by the i th magnetometer vector with the B line is given by, using Eq. (6),

$$\alpha_i(t) = \cos^{-1} \left\{ \frac{M_i(t)}{\sqrt{M_1^2(t) + \text{Max}^2 [M_2(t)]}} \right\}$$

where $\text{Max}[M_2(t)]$ is given in Eq. (8). This algorithm has its limitation, and will now be discussed. The term $\text{Max}[M_2(t)]$ is used in α_i formula because of necessity due to the unavailability of $M_3(t)$ data. If there is no spin vector movement, it has been shown [in Eq. (3)] that this term really equals the vector sum of the B components perpendicular to the spin axis. However, if the spin axis moves, then, as shown in Eq. (8), the term $\text{Max}[M_2(t)]$ becomes a not too simple combination of $M_2(t_0)$, $M_3(t_0)$, and even $M_1(t_0)$. The error in $\alpha_i(t)$ is given by

$$\Delta\alpha_1(t) = \cos^{-1} \left\{ \frac{M_1(t)}{\sqrt{M_1^2(0) + M_2^2(0) + M_3^2(0)}} \right\} - \cos^{-1} \left\{ \frac{M_1(t)}{\sqrt{M_1^2(t_m) + M_2^2(0) + \cos^2 \theta(t_m)}} \right. \\ \left. \frac{M_3^2(0) + \sin^2 \theta(t_m) M_1^2(0) - 2 \cos \theta(t_m) \sin \theta(t_m) M_1(0) M_3(0)}{\sqrt{M_3^2(0) + \sin^2 \theta(t_m) M_1^2(0) - 2 \cos \theta(t_m) \sin \theta(t_m) M_1(0) M_3(0)}} \right\}$$

(10)

which is time (t and t_m) dependent. For given values of $M_1(t)$, $M_1(0)$, and $\theta(t_m)$, the error $\Delta\alpha_1(t)$ can be computed, using Eq. (10). For a time span longer than a spin period, it is reasonable to expect that $\Delta\alpha_1(t)$ is distributed with its mean near zero. For Rocket A31.603, the value of $\langle \theta(t_m) \rangle \approx 18^\circ$. This can be observed from the variations of $\alpha_1(t)$ and $\alpha_2(t)$: in a period of $\alpha_2(t)$, which is the aspect angle of the magnetometer in spin plane, there are approximately 18° variations of $\alpha_1(t)$, which is the aspect angle of the magnetometer looking forward along the spin axis. If the values of all the terms in Eq. (10) are known, the error $\Delta\alpha_1(t)$ can be determined at any time t .

The realistic situation is more complicated, because the vehicle not only tumbles but it precesses in a large conic angle. In general, three Euler angles are needed for arbitrary rotations. Accordingly, Eq. (7) has to be modified to accommodate three rotation matrices on the right-hand side, and Eq. (10) becomes much more complicated. If such a detailed analysis is necessary, it can be done. However, if our objective is simply to estimate the range of error in determining $\alpha_1(t)$, Eq. (10) is believed to be adequate because Rocket A31.603 spins and tumbles only, almost. As pointed out in the previous paragraph, $\Delta\alpha_1(t)$ is expected to have its mean near zero, and for $\alpha_1(t)$, $\Delta\alpha_1(t)$ varies between $\pm 18^\circ$, with a standard deviation probably lying within $\pm 10^\circ$ for its sinusoidal behavior.

7. THE PROBLEM OF ATTITUDE DETERMINATION OF ROCKET AXIS

In this section, we determine the attitude of the rocket axis with respect to the local vertical coordinate system. For Rocket A31.603, magnetometer No. 1 looks forward along the spin axis, which is approximately the same as the geometrical axis of the rocket. If the spin axis deviates considerably from the geometrical axis, or if magnetometer No. 1 does not look along either axis, there would be a considerable source of error in the analysis. Nevertheless, even as a zeroth order approximation, let us try to derive as much information about the rocket attitude as possible, in order to gain an understanding of the behavior of the rocket.

Let us summarize what we know at this stage. By using two magnetometer data sets, the aspect angle $\alpha_1(t)$ between a magnetometer vector and the Earth's magnetic field vector \underline{B} at the position of the rocket is known approximately, at irregularly spaced instants, about 1 sec apart. The magnetic field vector \underline{B} is not sensitive to time and space variation for the duration and trajectory span of the rocket considered, and is, therefore, known with good accuracy. The problem now is whether one can determine the attitude (azimuth and elevation angles) of the rocket axis \underline{R} with respect to a local vertical coordinate system (x = east, y = north, z = local vertical, that is, zenith).

8. ZERO TH ORDER APPROXIMATION

Observation of $\alpha(t)$ variation against t shows that the aspect angle of the rocket axis varies between nearly -180° to nearly $+180^\circ$, implying that the rocket tumbles almost in a vertical plane. The deviation from the plane of motion is approximately varying at less than 15° . That is, the rocket precesses at a large cone angle, greater than 75° , so that it behaves almost like tumbling. From energy considerations, it is more favorable for a rocket to tumble in its trajectory plane than to wobble significantly out of its trajectory plane. A somewhat analogous situation is known in the theory of satellite boom dynamics, in which modes of boom oscillations in the equatorial plane^{5,6} of the dominant angular momentum of the system are energetically more favorable than those wobbling out of the equatorial plane.

As a zeroth order approximation, let us assume, for the time being, that the rocket tumbles in its vertical trajectory plane. This assumption, together with the knowledge of $\alpha_1(t)$, enables us to constrain the possible direction of the rocket axis from those lying anywhere in a cone to only two directions, the intersections of the α -cone with the vertical plane. Now, we have obtained two sets of solutions, at all times t .

To decide which solution is the correct one at time t , we require that: (1) the solution can be traced back continuously to the initial time t_0 , so that the two sets of solutions can be distinctly identified, and (2) the set that does satisfy the initial condition is the correct one. The initial condition is at time t_0 , when the rocket starts to tumble, due to the separation of its booster. At that moment, the rocket is still pointing along its velocity vector. For Rocket A31.603, we have found that one of the two sets of solutions satisfies the initial condition exactly. This

-
5. Lai, S. T., and Bhavnani, K. H. (1975) Dynamics of Satellite Wire-Boom Systems, AFCRL-TR-75-v220, AD A014859.
 6. Lai, S. T., Mahon, R., and Smidley, M. (1979) Dynamics of wire boom oscillations on a spinning satellite, J. Appl. Math. Phys. 30:1-29.

encouraging result leads one to have confidence on the correctness of the selection of the solution sets, and to carry on further for refinement of results.

9. ROCKET ELEVATION AND AZIMUTH ANGLES

We define the azimuth ϕ and elevation θ angles in a local vertical coordinate system as in Figure 1.

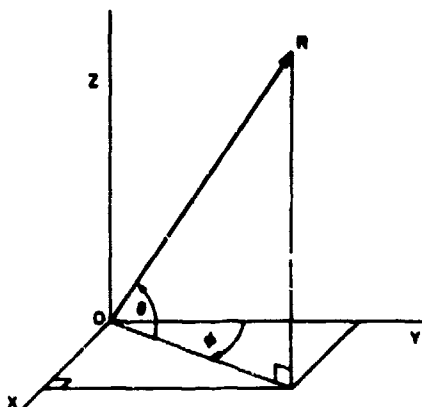


Figure 1. Local Vertical Coordinate System

OR is the vector of the rocket axis. In vector notation, we write the unit vector:

$$\hat{R} = (\cos \theta \sin \phi, \cos \theta \cos \phi, \sin \theta). \quad (11)$$

Similarly, the magnetic field vector \hat{B} can be written as

$$\hat{B} = (\cos I \sin D, \cos I \cos D, \sin I) \quad (12)$$

where I is the inclination angle and D the dip angle. The cap ^ denotes unit vector. At White Sands where the rocket considered was launched, $I = 60^\circ$ and $D = 11^\circ$. Also, at launch time, it is known that $\phi = 33.5^\circ$ eastward from north. It is believed that this angle should remain unchanged until the booster separates at $t_0 = 64$ seconds.

Since the rocket tumbles in an approximately vertical plane, the variation $\text{Max}|\phi - \langle \phi \rangle|$ should be small compared to the variation of θ in a tumble period. For the rocket considered, the ratio of such variations is less than 10%. Thus, the angle ϕ behaves almost like a constant, while the angle θ varies.

From Eqs. (11) and (12), the angle α between the magnetic field vector \hat{B} and the rocket axis vector \hat{R} is given by

$$\cos \alpha = \underline{\mathbf{B}} \cdot \underline{\mathbf{R}} = \cos \theta \cos I \cos(\phi - D) + \sin \theta \sin I. \quad (13)$$

The closest encounter between B and R occurs when

$$\frac{\partial \cos \alpha}{\partial \theta} = 0 \quad (14)$$

which gives the condition:

$$\tan \theta = \frac{\tan I}{\cos(\phi - D)}. \quad (15)$$

Substituting Eq. (15) into Eq. (13), we have

$$\cos \alpha_{\min} = \left\{ \cos^2 I \cos^2(\phi - D) + \sin^2 I \right\}^{1/2}$$

and

$$\phi = D \pm \cos^{-1} \left\{ \left[\cos^2 \alpha_{\min} - \sin^2 I \right]^{1/2} / \cos I \right\}. \quad (16)$$

In Eq. (16), there are two sets of solutions. We can choose the set that varies around the initial value at $t = t_0$, where $\phi = 33.5^\circ$. Thus, this technique gives the values of ϕ at the moments of closest encounter between B and R, that is, when α_1 is minimum.

For the rocket considered, there are only six moments of B and R closest encounter. Together with the initial value of t_0 , we have seven data points to be fitted by a sine curve with tumble frequency. The fitted function gives $\phi(t)$ at all times. Then, using Eq. (13), the angle $\theta(t)$ can be calculated at all points. This determines the elevation and azimuth angles of the rocket at all points (Figure 2). The results are listed in Appendix A.

In practice there is noise in the data, which should be smoothed by curve-fitting or other filtering techniques before the method of closest encounter can be applied.

10. MOON DIRECTION

To calculate the elevation (ϵ) and the azimuth (λ) of the moon at the time of rocket flight, we use the data in Table 1.

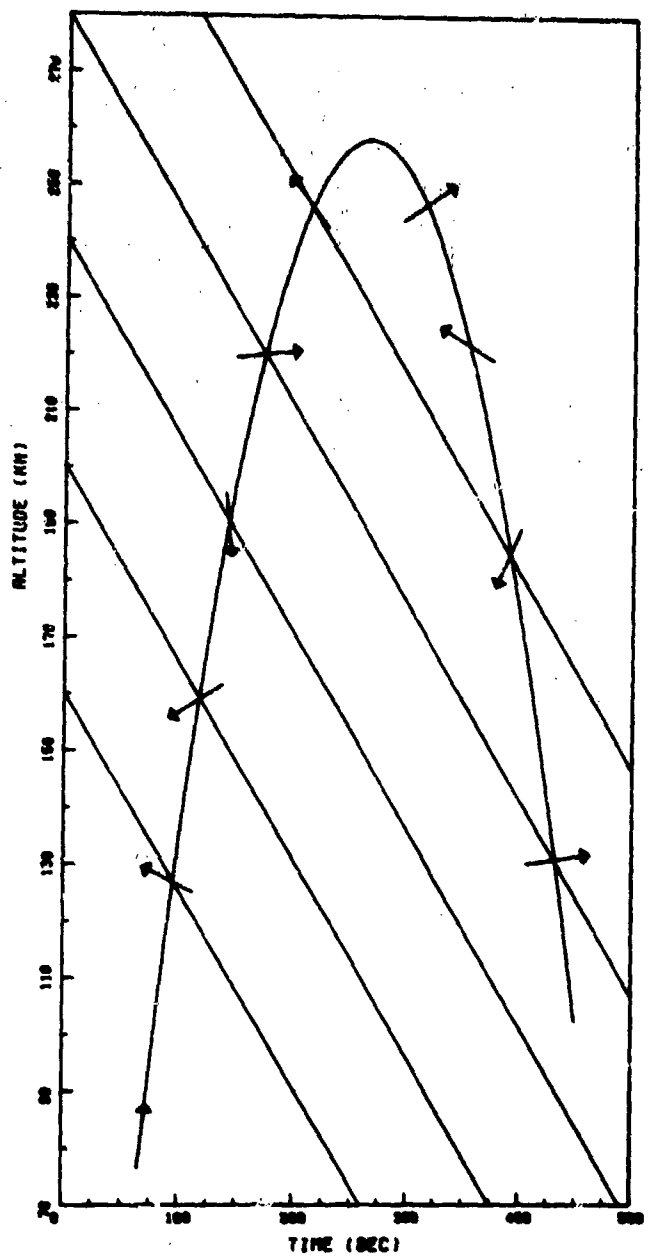


Figure 2. Rocket Attitude in the Plane of Rocket Trajectory. Magnetic field lines are represented by the long straight lines

Table 1. Ephemeris Data of Moon and Launch Site

	Moon	Greenwich	White Sands
	5 ^h 54 ^m 04 ^s	17 ^h 11 ^m 11 ^s	10 ^h 5 ^m 11 ^s
Right Ascension			
Declination	18. 475°	-----	32. 5°

The right ascension values $5^{\text{h}} 54^{\text{m}} 04^{\text{s}} = 33.5^{\circ}$, and $10^{\text{h}} 5^{\text{m}} 11^{\text{s}} = 151.3^{\circ}$. In a coordinate system, E, in which x = south, y = east (both on the equatorial plane), and z = north star, the direction cosines of zenith $\hat{\xi}$ vector is

$$\hat{\xi} = (\cos 32.5^{\circ}, 0, \sin 32.5^{\circ})$$

and that of moon $\hat{\mu}$ vector is

$$\hat{\mu} = (\cos \delta \cos \psi, \cos \delta \sin \psi, \sin \delta)$$

where

$$\psi = -10^{\text{h}} 5^{\text{m}} 11^{\text{s}} + 5^{\text{h}} 54^{\text{m}} 04^{\text{s}} = -62.8^{\circ}$$

$$\delta = 18.475^{\circ}.$$

In a local vertical system, L, in which x = south, y = east, and z = zenith, a vector $\hat{\mu}$ defined in E system becomes matrix transformed by a rotation about -y-axis of L-system. That is

$$\begin{aligned} [\hat{\mu}]_L &= \begin{bmatrix} \sin 32.5^{\circ} & 0 & -\cos 32.5^{\circ} \\ 0 & 1 & 0 \\ \cos 32.5^{\circ} & 0 & \sin 32.5^{\circ} \end{bmatrix} \begin{bmatrix} \cos \delta & \cos \psi \\ \cos \delta & \sin \psi \\ \sin \delta \end{bmatrix} \\ &= \begin{bmatrix} -0.034 \\ -0.843 \\ -0.536 \end{bmatrix}. \end{aligned}$$

The elevation angle (ϵ), measured from the local horizon, and the azimuth angle (λ), measured clockwise from the east, are then obtained by equating

$$\hat{\mu} = \begin{bmatrix} \cos \epsilon & \sin \lambda \\ \cos \epsilon & \cos \lambda \\ \sin \epsilon \end{bmatrix} = \begin{bmatrix} -0.034 \\ -0.843 \\ 0.536 \end{bmatrix}$$

which yields

$$\left\{ \begin{array}{l} \epsilon = 32.4^{\circ} \\ \lambda = 182.3^{\circ} \end{array} \right. . \quad (17)$$

The results in Eq. (17) have been confirmed, within a half degree, by using AFGL's standard computer program SOLUN. They do not, however, agree with the numbers given by Chamberlain⁷ and by Sluder and Kofsky.⁸

Using the rocket attitude data and the moon direction [Eq. (17)], the angle $\beta(t)$ between the rocket axis \hat{R} and the moon $\hat{\mu}$ at time t can be calculated (Figure 3). According to design, the moon can not be seen unless $\beta(t)$ lies between 30° and 44° (for backward view) or between 176° and 190° (for forward view) (see Figure 4).

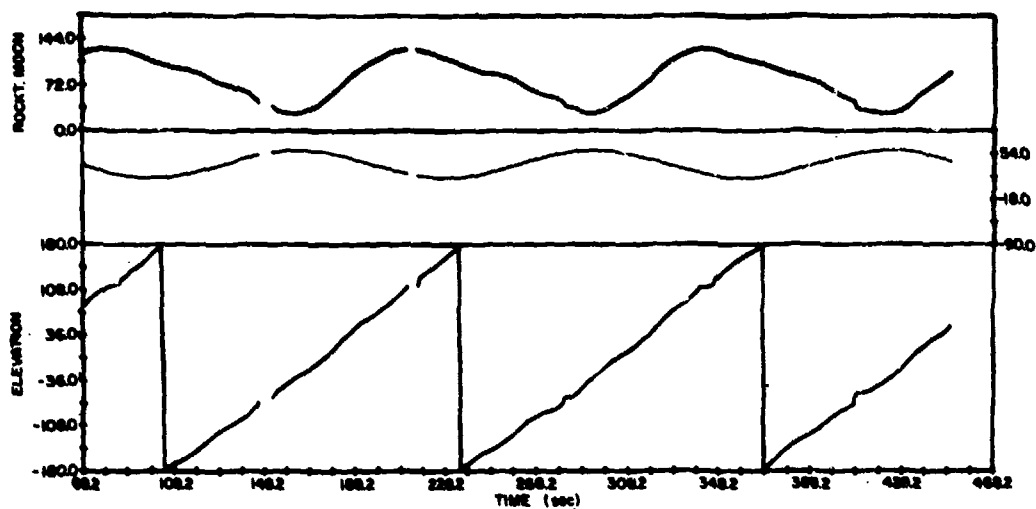


Figure 3. Rocket Elevation Angle, Azimuth Angle, and the Angle Between Rocket and Moonlight

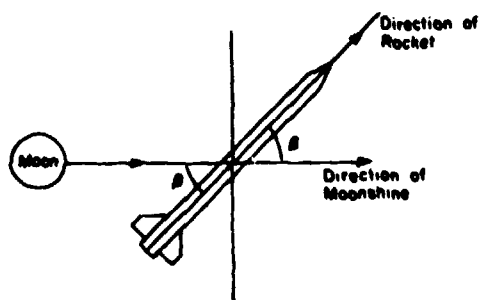


Figure 4. Relation of Rocket and Moonshine Directions. This figure can almost be regarded as looking down from zenith, and the moonshine projection is in west-east direction

-
7. Chamberlain, M.T. (1979) Data Analysis of Film From AFGL Rocket A31, 603, AFGL-TR-79-0195, AD A092705.
 8. Sluder, R.B., and Kofsky, I.L. (1978) Photographic Measurements of Electrical Discharges, AFGL-TR-78-0082, AD A058469.

The range of moon viewing β values should be considerably wider than those specified by design. The uncertainties are due to: (1) α angle as computed by using two magnetometers, (2) spin axis deviation from rocket axis, (3) noise in data, (4) approximation in the theory of \hat{B} and \hat{R} close encounter, and (5) too few points available in the close encounter curve fitting. The uncertainty due to source (1) has been estimated in Section 6. Let us put up a rough figure for the combined uncertainty: $\pm 20^\circ$, as an educated guess only, unless someone can give a reason to indicate otherwise.

The moon view times are taken from Chamberlain⁷ and are given in column 1 of Table 2. The magnetic aspect angles $\alpha(t)$ are given in column 2. The computed elevation and azimuth angles of the rocket in a (east, north, zenith) coordinate system are given in columns 3 and 4. The angles $\beta(t)$ between the moonshine vector and rocket vector are given in column 5.

Table 2. Rocket Attitude Angles During Moon View Times

Moon View Time, sec	Magnetic Aspect Angle $\alpha(t)$	Rocket Elevation	Rocket Azimuth	Angle $\beta(t)$ Between Rocket and Moon
125.1	65.6°	-125.5°	31.1°	79.5°
159.5	36.8°	-39.3°	58.1°	26.6°
266.2	36.7°	-97.5°	43.1°	62.8°
406.3	21.2°	-75.3°	52.9°	46.3°

Since the moonshine is almost in west to east direction, dipping downwards, it is reasonable that the rocket should lie in a south-west to north-east direction, dipping downwards, in order for the camera on the rocket to view the moon. Qualitatively, the rocket elevation and azimuth angles as shown in Table 2 satisfy this criterion. As for the angle β between the rocket and the moon, the last three numbers fall in the range $(30^\circ, 44^\circ) \pm 20^\circ$, as they should. The first β angle lies just outside this range. In no time is the moon seen in a forward view.

References

1. Cohen, H. A., Sherman, C., and Mullen, G. (1979) Spacecraft charging due to positive ion emission: an experimental study, Geophys. Res. Lett. 6(No. 6):515.
2. Winckler, J. R. (1980) The application of artificial electron beams to magnetospheric research, Review of Geophysics and Space Physics, 18:659-682.
3. Jacobsen, T. A., and Maynard, N. C. (1980) Polar 5-an electron accelerator experiment within an aurora 3. Evidence for significant spacecraft charging by an electron accelerator at ionospheric altitudes, Planet. Sp. Sci. 28:291-307.
4. SUA/AFGL (1979) Data Report Rocket No. A31. S03.
5. Lai, S. T., and Bhavrani, K. H. (1975) Dynamics of Satellite Wire-Boom Systems, AFCRL-TR-75-0220, AD A014859.
6. Lai, S. T., Mahon, H., and Smiddy, M. (1979) Dynamics of wire-boom oscillations on a spinning satellite, J. Appl. Math. Phys. 30:1-29.
7. Chamberlain, M. T. (1979) Data Analysis of Film From AFGL Rocket A31. 603, AFGL-TR-79-0185, AD A092705.
8. Sluder, R. B., and Kofsky, I. I. (1978) Photographic Measurements of Electrical Discharges, AFGL-TR-78-0082, AD A058469.

Appendix A

Attitude Data of Rocket No. A31.003

Column 1 shows universal time starting from the moment of booster separation. Column 2 lists magnetic pitch angles [ref. 2]. Columns 3 and 4 are calculated elevation and azimuth angles in the local vertical coordinate system. Column 5 gives the calculated moon pitch angles.

TIME SEC.	R.A. DEG.	ELV DEG.	AZIMUTH DEG.	R. MOON DEG.	POINT NO.
68.20	142.66	82.18	33.31	117.99	1
68.48	144.34	83.98	32.67	119.11	2
69.48	146.09	85.64	32.04	120.23	3
70.80	147.90	87.77	31.41	121.32	4
70.66	149.81	89.80	30.78	122.47	5
72.00	154.95	95.76	29.34	124.96	6
73.40	156.91	99.49	27.73	126.52	7
74.48	161.54	102.29	26.94	127.33	8
75.20	163.29	104.16	26.17	127.73	9
76.00	164.89	105.86	25.41	128.01	10
76.48	165.57	106.59	25.04	128.09	11
76.80	166.29	107.35	24.67	128.16	12
77.40	167.20	108.31	24.13	128.20	13
78.00	167.86	109.98	23.60	128.16	14
78.40	169.07	110.34	23.25	128.28	15
79.00	170.29	111.77	22.73	128.33	16
79.50	171.44	113.03	22.23	128.27	17
80.40	172.77	114.61	21.58	128.15	18
83.00	173.86	115.33	19.62	127.36	19
83.40	174.07	115.51	19.34	127.24	20
84.00	174.40	115.80	18.93	127.07	21
84.60	174.75	116.12	18.54	126.90	22
85.00	174.97	116.32	18.29	126.79	23
86.00	173.97	124.85	17.68	125.97	24
86.60	173.07	128.01	17.34	125.62	25
87.40	171.22	128.14	16.91	125.04	26
88.00	170.05	129.43	16.51	124.52	27
89.20	166.46	133.21	16.06	123.46	28
90.40	160.33	139.46	15.57	121.42	29
91.00	157.64	142.21	15.09	120.18	30
92.60	155.50	144.37	14.66	119.37	31
93.20	153.67	146.21	14.71	118.48	32
93.80	152.17	147.73	14.58	117.80	33
94.20	151.03	148.57	14.50	117.61	34
94.60	150.66	149.74	14.43	117.09	35
95.60	146.67	153.45	14.29	115.24	36
96.20	144.42	155.51	14.23	114.30	37
96.80	142.48	157.46	14.19	113.39	38
97.60	139.65	159.29	14.17	112.06	39
99.20	137.55	162.39	14.17	111.36	40
99.00	134.31	165.62	14.21	119.51	41
100.00	130.44	169.50	14.30	107.62	42
101.40	125.90	174.04	14.51	105.47	43
102.60	122.66	177.26	14.77	103.91	44
104.00	118.14	-178.27	15.17	101.77	45

TIME SEC.	R.B DEG.	ELV DEG.	AZIMUTH DEG.	R.MOON DEG.	POINT NO.
105.00	115.62	-175.72	15.51	100.65	46
105.00	113.81	-173.92	15.82	99.89	47
106.00	112.20	-172.33	16.17	99.26	48
107.40	110.53	-170.87	16.54	98.62	49
108.20	106.86	-169.92	16.94	97.99	50
109.00	107.25	-167.43	17.37	97.48	51
109.00	105.77	-165.97	17.83	96.91	52
110.40	104.66	-164.88	18.19	96.55	53
111.20	103.25	-163.80	18.78	96.12	54
112.20	101.31	-161.81	19.37	95.62	55
113.40	98.99	-159.34	20.23	94.78	56
114.60	96.48	-156.81	21.14	93.99	57
115.00	93.03	-154.31	22.11	93.04	58
117.00	90.84	-151.20	23.12	91.79	59
118.00	87.89	-148.52	24.00	90.68	60
118.40	86.74	-147.40	24.35	90.20	61
119.00	85.01	-145.71	24.90	89.46	62
119.00	82.72	-143.48	25.65	88.49	63
120.60	80.18	-140.91	26.41	87.27	64
121.40	77.47	-138.36	27.10	86.03	65
122.00	75.51	-136.42	27.78	85.09	66
123.00	72.24	-133.22	28.78	83.48	67
124.20	68.39	-129.45	30.00	81.55	68
125.40	64.54	-125.67	31.25	79.95	69
127.20	58.20	-119.50	33.15	76.98	70
129.20	53.48	-114.79	35.29	73.93	71
130.60	50.17	-111.52	36.79	71.66	72
131.40	48.75	-110.13	37.55	70.90	73
132.00	47.87	-109.27	38.30	70.45	74
132.60	46.97	-108.39	38.34	69.96	75
133.40	45.28	-106.70	39.79	68.93	76
135.00	42.16	-103.52	41.48	66.93	77
136.40	39.51	-100.77	42.93	65.13	78
137.60	37.34	-98.46	44.15	63.57	79
138.00	35.24	-96.16	45.35	61.97	80
140.20	32.53	-93.06	46.70	59.75	81
141.40	29.63	-90.47	47.33	57.85	82
142.20	27.46	-86.77	48.56	55.07	83
142.80	25.80	-84.40	49.09	53.75	84
143.20	24.66	-82.49	49.44	52.09	85
144.00	22.19	-79.51	50.13	49.05	86
145.00	21.29	-76.45	50.36	47.48	87
145.80	19.42	-71.47	51.59	43.74	88
147.00	18.17				
149.20	17.82				
150.60	16.89				
152.00	21.77	-62.25	55.70	36.08	92
154.00	26.01	-52.26	56.67	31.11	93

TIME SEC.	R.D DEG.	ELV DEG.	AZIMUTH DEG.	R.NOON DEG.	POINT NO.
199.20	27.09	-49.57	57.16	29.71	94
196.40	30.00	-46.59	57.58	26.41	95
196.00	30.99	-45.30	57.70	27.97	96
196.00	33.86	-41.67	56.82	26.92	97
199.00	35.76	-39.33	56.24	26.46	98
199.00	37.72	-36.94	56.46	26.22	99
199.00	40.96	-33.84	56.54	26.35	100
191.40	43.49	-30.84	56.39	26.87	101
182.60	43.49	-27.78	56.56	27.49	102
183.60	45.48	-26.42	56.51	27.98	103
184.40	46.54	-25.74	56.47	26.25	104
184.00	47.11	-23.05	56.33	29.16	105
185.00	48.69	-22.02	56.22	29.89	106
186.40	50.24	-19.02	56.05	21.14	107
187.20	52.11	-16.73	57.67	33.16	108
188.00	54.69	-13.46	57.27	35.39	109
189.00	57.43	-9.76	56.71	36.97	110
171.20	60.42	-6.77	56.16	40.63	111
172.40	63.11	-3.36	55.54	43.46	112
173.60	66.01	.81	54.73	47.08	113
175.00	69.57	7.23	53.44	50.42	114
176.20	72.79	9.19	53.02	52.60	115
177.00	75.18	11.02	52.58	56.30	116
178.20	78.37	14.70	51.83	59.57	117
179.20	81.59	17.68	51.20	62.42	118
180.00	84.21	20.00	50.71	64.55	119
180.60	86.25	23.17	50.04	67.43	120
181.40	89.00	26.89	49.18	70.96	121
182.40	92.36	31.58	47.92	75.41	122
183.00	96.49	35.70	46.80	79.29	123
185.00	100.13	40.63	45.45	83.90	124
186.40	104.34	42.75	44.86	85.87	125
187.00	106.44	44.19	44.46	87.19	126
187.40	107.73	47.47	43.45	90.22	127
188.40	110.67	49.14	42.83	91.79	128
189.00	112.15	50.84	42.21	93.37	129
189.60	113.67	53.53	41.38	95.78	130
190.40	116.10	56.33	39.26	100.20	131
192.40	120.39	60.00	38.41	101.73	132
193.20	121.87	61.95	37.33	103.51	133
194.20	123.61	66.21	35.61	107.07	134
195.80	127.52	69.70	34.32	109.14	135
197.00	129.80	71.06	33.04	111.03	136
198.20	131.97	74.07	31.56	113.30	137
199.60	134.77				138

TYPE SEC.	R.B DEG.	ELV DEG.	AZIMUTH DEG.	R.POCN DEG.	POINT NO.
200.20	136.19	75.57	30.34	114.35	139
200.00	138.00	77.40	30.31	115.61	140
201.20	139.25	78.79	29.90	116.44	141
202.00	141.76	81.42	29.00	118.04	142
202.40	143.02	82.74	28.50	118.81	143
203.00	140.02	87.94	27.20	121.54	144
203.80	137.51	87.79	24.65	125.42	145
204.00	161.59	102.03	23.38	126.53	146
204.20	165.21	105.02	22.36	127.10	147
210.40	168.71	109.54	21.38	127.52	148
211.20	170.96	112.01	20.76	127.60	149
213.00	178.89				
214.60	176.49				
215.00	173.96	114.70	17.84	126.32	152
216.00	171.54	127.76	17.10	125.21	153
217.00	169.42	130.03	16.59	124.49	154
220.00	161.60	138.21	15.34	121.63	155
221.00	158.67	141.18	15.02	120.47	156
222.20	157.61	142.25	14.90	120.03	157
223.00	155.54	144.28	14.70	119.18	158
224.20	152.20	147.70	14.46	117.71	159
225.20	149.36	150.56	14.31	116.46	160
226.20	146.70	153.23	14.22	115.27	161
227.40	143.45	156.48	14.17	113.81	162
228.40	140.98	158.98	14.19	112.69	163
229.40	138.14	161.88	14.26	111.42	164
230.00	136.35	163.58	14.33	110.61	165
230.40	135.20	164.74	14.38	110.10	166
230.80	134.07	165.86	14.45	109.59	167
231.60	131.49	168.44	14.60	108.42	168
232.60	128.16	171.76	14.84	106.90	169
233.40	125.60	174.31	15.06	105.74	170
234.20	122.89	177.02	15.32	104.51	171
235.40	118.97	-179.08	15.76	102.74	172
236.40	115.53	-175.66	16.19	101.18	173
237.60	111.32	-171.48	16.76	99.26	174
238.40	108.59	-168.76	17.18	98.02	175
239.60	105.10	-165.30	17.86	96.54	176
240.80	101.72	-161.96	18.60	95.13	177
241.80	99.15	-159.44	19.27	94.12	178
242.60	96.61	-156.94	19.97	93.13	179
243.40	95.13	-155.48	20.41	92.56	180
244.60	93.65	-154.03	20.87	92.00	181
245.00	91.19	-151.62	21.66	91.06	182
245.80	89.64	-150.12	22.31	90.57	183
246.60	88.21	-148.75	22.99	90.16	184
247.40	86.77	-147.36	23.68	89.74	185

TIME SEC.	R.B DEG.	ELV DEG.	AZIMUTH DEG.	F.MOON DEG.	POINT NO.
248.20	85.32	-145.97	24.40	89.32	186
249.00	83.85	-144.57	25.13	88.87	187
250.20	81.58	-142.39	26.26	88.15	188
251.60	78.79	-139.72	27.63	87.19	189
252.80	76.04	-137.07	28.83	86.09	190
254.20	72.65	-133.81	30.26	84.64	191
255.40	69.50	-130.76	31.51	83.16	192
256.00	67.87	-129.18	32.14	82.35	193
256.60	66.20	-127.56	32.78	81.51	194
257.20	64.14	-125.53	33.41	80.37	195
259.20	58.05	-119.54	35.56	76.96	196
260.20	55.07	-116.59	36.53	75.21	197
261.20	51.93	-113.46	37.71	73.29	198
262.60	47.48	-108.97	39.21	70.44	199
263.80	43.57	-104.94	40.48	67.79	200
265.00	39.43	-100.58	41.74	64.84	201
266.20	36.59	-97.54	42.98	62.79	202
267.40	34.55	-95.30	44.20	61.27	203
267.80	33.91	-94.59	44.60	60.78	204
268.60	32.55	-93.04	45.40	59.69	205
269.20	31.71	-92.07	45.98	59.00	206
270.00	30.38	-90.47	46.75	57.84	207
271.40	28.29	-87.82	48.06	55.89	208
272.20	27.19	-86.33	48.78	54.78	209
273.40	26.16	-84.83	49.83	53.62	210
274.60	25.24	-83.37	50.83	52.47	211
275.40	24.71	-82.47	51.48	51.74	212
276.60	23.79	-80.75	52.40	50.38	213
277.80	22.69	-78.45	53.26	48.57	214
278.60	21.91	-76.50	53.91	47.05	215
279.20	21.29	-74.60	54.20	45.60	216
279.80	20.65	-71.88	54.58	43.58	217
280.60	20.85	-63.05	55.17	37.56	218
281.80	21.09	-116.94	55.72	80.61	219
282.40	21.24	-63.03	56.03	37.24	220
283.20	21.58	-62.28	56.42	36.64	221
284.20	22.19	-60.82	56.86	35.57	222
285.40	23.94	-56.87	57.32	33.08	223
286.20	25.16	-54.64	57.59	31.76	224
288.20	29.82	-47.38	58.13	28.31	225
289.00	31.81	-44.63	58.29	27.37	226
289.60	33.68	-42.14	58.38	26.74	227
290.80	37.23	-37.64	58.52	26.15	228
291.80	39.45	-34.91	58.58	26.15	229
292.60	41.42	-32.52	58.58	26.40	230

TYPE SEC.	R.H. DEG.	EL.V DEG.	AZIMUTH DEG.	R.MOON DEG.	POINT NO.
293.40	44.03	-29.79	58.56	27.05	231
294.00	45.93	-27.14	58.52	27.73	232
294.60	47.86	-24.75	58.44	28.61	233
295.00	50.24	-22.06	58.29	29.92	234
296.00	52.97	-19.87	58.08	31.48	235
296.40	57.30	-13.83	57.65	34.59	236
299.40	60.01	-10.69	57.32	37.17	237
300.00	63.32	-6.81	56.77	40.16	238
301.00	65.57	-4.17	56.32	42.35	239
302.40	66.93	-2.57	56.03	43.71	240
303.00	68.21	-1.06	55.72	45.02	241
304.00	70.27	1.30	55.17	47.22	242
304.60	71.47	2.01	54.82	48.53	243
305.20	72.60	4.17	54.45	49.80	244
306.40	74.83	6.85	53.67	52.37	245
307.20	76.24	8.56	53.12	54.05	246
309.40	78.27	11.03	52.25	56.52	247
309.20	79.76	12.87	51.63	58.30	248
310.00	81.67	15.06	51.10	60.44	249
311.20	84.48	18.35	50.00	63.63	250
312.00	86.32	20.50	49.31	65.74	251
313.00	88.79	23.37	48.42	68.53	252
313.80	91.04	25.93	47.69	70.98	253
314.60	93.81	29.04	46.94	73.86	254
314.00	94.50	29.81	46.75	74.58	255
315.40	95.77	31.20	46.18	76.05	256
315.80	96.34	31.90	45.79	76.81	257
316.20	96.93	32.69	45.40	77.50	258
316.80	97.80	33.76	44.81	78.77	259
317.40	99.51	35.67	44.20	80.54	260
317.80	100.92	37.24	43.00	81.98	261
318.80	104.50	41.18	42.78	85.56	262
319.00	108.05	45.09	41.74	89.09	263
320.80	111.67	49.04	40.69	92.59	264
321.60	115.38	53.07	39.63	96.10	265
322.00	119.22	57.22	38.57	99.62	266
323.80	122.65	60.93	37.49	102.72	267
324.00	126.09	64.63	36.42	105.72	268
325.80	128.88	67.65	35.34	108.14	269
326.40	130.49	69.38	34.70	109.50	270
326.80	131.59	70.56	34.27	110.40	271
327.20	132.70	71.75	33.84	111.30	272
327.80	134.41	73.58	33.20	112.63	273
328.80	137.39	76.74	32.14	114.84	274
80	142.72	82.38	30.05	118.46	275

TYPE SEC.	R.B DEG.	ELV DEG.	AZIMUTH DEG.	E. POIN DEG.	POINT NO.
331.80	145.17	84.95	29.03	119.95	276
332.80	147.68	27.58	28.03	121.34	277
333.80	150.41	29.57	27.04	122.30	278
334.80	153.42	23.56	26.07	124.01	279
335.80	156.41	96.67	25.13	125.12	280
336.80	159.73	100.12	24.22	126.14	281
337.40	162.02	102.57	23.69	126.72	282
337.80	163.72	104.31	23.34	127.10	283
338.40	165.33	106.01	22.82	127.35	284
338.80	167.48	108.35	22.48	127.70	285
339.20	169.86	111.03	22.15	128.00	286
342.80	171.28	112.08	19.61	127.17	287
344.80	173.40	114.34	18.10	126.69	288
345.40	174.60	115.85	17.74	126.55	289
345.80	175.02	116.06	17.51	126.45	290
346.40	174.62	124.27	17.18	125.75	291
346.80	173.58	125.56	16.37	125.47	292
347.80	171.01	128.46	16.47	124.71	293
348.80	168.42	131.22	16.01	123.88	294
349.80	164.45	135.30	15.51	122.63	295
350.80	160.93	138.89	15.25	121.36	296
351.80	158.14	141.72	14.95	120.24	297
352.80	155.69	144.21	14.59	119.19	298
354.00	152.37	147.53	14.46	117.77	299
355.00	142.37	157.56	14.18	113.33	300
359.20	139.30	160.67	14.27	111.98	301
360.00	137.56	162.37	14.36	111.23	302
360.80	135.89	164.04	14.49	110.53	303
361.60	134.20	165.72	14.55	110.93	304
362.60	132.13	167.79	14.93	110.11	305
363.40	130.38	169.57	15.14	108.32	306
364.20	128.53	171.36	15.41	107.59	307
365.00	126.75	173.13	15.70	106.91	308
365.60	125.16	174.71	15.95	106.28	309
366.40	123.10	176.75	16.30	105.44	310
367.20	120.97	178.91	16.58	104.62	311
368.20	117.65	-177.84	17.20	103.24	312
369.00	115.11	-175.33	17.35	102.19	313
369.60	113.00	-173.32	18.01	101.77	314
370.00	111.76	-172.01	18.25	100.77	315
371.40	110.45	-171.71	18.51	100.32	316
370.80	109.15	-169.42	18.76	99.64	317
371.20	107.78	-168.07	19.03	99.14	318
372.00	104.94	-165.26	19.58	97.85	319
372.80	102.14	-162.40	20.15	96.63	320

TIME SEC.	R.R DEG.	FLV DEG.	AZIMUTH DEG.	R.MOON DEG.	POINT NO.
373.60	98.98	-150.37	20.75	95.19	321
374.20	96.54	-156.06	21.22	94.05	322
375.00	93.31	-153.77	21.86	92.54	323
375.60	91.41	-151.91	22.35	91.72	324
376.20	89.52	-150.05	22.96	90.99	325
376.80	87.63	-148.20	23.38	90.07	326
377.60	85.17	-145.79	24.08	89.07	327
378.00	83.95	-144.59	24.45	88.48	328
378.80	81.51	-142.21	25.18	87.38	329
379.40	79.75	-140.49	25.74	86.61	330
379.80	78.60	-139.37	26.12	86.10	331
380.40	76.87	-137.68	26.70	85.32	332
380.80	75.71	-136.55	27.09	84.80	333
381.20	74.70	-135.57	27.48	84.36	334
381.80	73.41	-134.73	28.07	83.96	335
382.00	72.98	-133.92	28.27	83.69	336
382.60	71.61	-132.60	28.88	83.12	337
383.00	71.69	-131.70	29.28	82.72	338
383.40	69.79	-130.84	29.69	82.34	339
384.20	67.98	-129.12	30.52	81.55	340
385.20	65.79	-128.99	31.56	80.59	341
386.00	64.39	-125.66	32.41	80.04	342
386.80	62.97	-124.31	32.25	79.45	343
387.60	61.39	-122.89	34.11	78.73	344
388.60	59.31	-121.79	35.18	77.72	345
389.40	57.60	-119.14	36.04	76.84	346
390.20	56.85	-117.43	36.90	75.91	347
391.20	55.56	-115.19	37.97	74.61	348
392.00	51.59	-113.24	38.83	73.44	349
392.40	50.58	-112.23	39.26	72.82	350
393.20	48.29	-109.92	41.11	71.34	351
393.80	46.04	-107.61	40.74	69.78	352
394.60	43.65	-105.14	41.58	68.13	353
395.40	41.44	-102.82	42.42	66.57	354
396.00	39.91	-101.22	43.03	65.48	355
396.80	37.63	-98.99	43.85	63.97	356
397.60	35.15	-96.03	44.85	61.84	357
399.40	33.48	-94.13	45.45	60.43	358
399.80	32.34	-92.81	45.84	59.54	359
400.40	31.07	-91.31	46.42	58.45	360
400.00	30.03	-90.03	46.39	57.52	361
400.80	28.00	-87.46	46.74	55.63	362
401.60	26.10	-84.88	48.47	52.74	363
402.40	25.03	-83.24	48.18	52.53	364
403.20	24.94	-83.05	49.87	52.31	365

TYPE SEC.	R.R. DEG.	ELV DEG.	AZIMUTH DEG.	R.MOCN DEG.	POINT NO.
404.80	23.08	-79.80	51.20	49.82	366
406.80	21.26	-75.47	52.73	46.49	367
407.40	21.05	-74.64	53.16	45.83	368
408.00	21.23	-59.08	53.57	35.94	369
408.60	22.88	-55.63	53.97	34.05	370
409.60	23.27	-55.45	54.61	33.65	371
410.60	23.50	-124.40	55.20	87.02	372
411.20	23.93	-55.06	55.54	33.00	373
412.40	25.11	-53.40	56.16	31.90	374
413.40	26.07	-52.11	56.52	31.07	375
414.20	26.75	-51.26	56.96	30.51	376
414.80	26.96	-51.03	57.12	30.33	377
414.80	27.07	-50.92	57.19	30.24	378
415.60	28.42	-49.00	57.48	29.30	380
415.00	29.07	-48.11	57.61	28.90	381
416.80	30.84	-46.85	57.84	28.32	382
417.20	30.72	-45.94	57.95	27.97	383
418.40	33.00	-42.96	58.22	27.02	384
418.80	73.55	-42.26	58.29	26.93	385
419.80	35.14	-40.27	58.44	26.41	386
420.80	36.71	-38.31	58.54	26.16	387
421.40	37.84	-36.09	59.57	26.09	388
422.00	39.05	-35.41	58.58	26.11	389
422.80	41.03	-32.98	58.57	26.34	390
423.80	43.58	-29.89	58.51	26.96	391
425.60	51.59	-20.42	58.07	30.88	392
427.40	53.72	-17.92	57.87	32.34	393
429.00	55.42	-15.94	57.70	33.59	394
429.60	57.10	-13.98	57.51	34.93	395
429.40	59.56	-11.14	57.23	36.91	396
429.80	60.90	-9.60	57.08	38.04	397
430.60	63.55	-6.55	56.75	40.36	398
431.60	66.77	-2.85	56.30	43.32	399
432.40	69.30	.04	55.91	45.73	400
433.60	73.02	4.31	55.26	49.41	401
434.80	76.69	8.51	54.55	53.13	402
435.80	79.53	11.78	53.31	56.12	403
436.20	80.65	13.07	53.64	57.71	404
436.60	81.78	14.37	53.37	58.51	405
437.00	82.91	15.67	53.09	59.72	406
437.40	83.80	16.81	52.80	60.91	407
439.00	85.38	18.54	52.36	62.46	408
438.80	87.40	20.87	51.75	64.69	409
439.20	88.37	22.00	51.44	65.78	410
439.80	89.77	23.63	50.96	67.38	411
440.40	91.18	25.27	50.46	68.97	412
440.80	92.13	26.37	50.13	70.24	413
441.80	94.27	28.88	49.27	72.53	414
442.60	95.84	30.72	48.56	74.40	415
443.80	97.54	32.81	47.46	76.63	416
445.00	100.11	35.70	46.32	79.60	417
446.80	104.72	41.02	44.56	84.67	418
448.40	109.15	45.99	42.93	89.27	419
448.80	110.28	47.25	42.52	90.44	420
449.40	112.41	49.59	41.90	92.52	